JACS
JOURNAL OF THE AMERICAN CHEMICAL SOCIETY

COMMUNICATION

pubs.acs.org/JACS

# Size of Elementary Clusters and Process Period in Silver Nanoparticle Formation

Masafumi Takesue,*[,†] Takuya Tomura,[†] Mitsuru Yamada,[†] Katsuhiko Hata,[†] Shigeo Kuwamoto,[‡] and Tetsu Yonezawa[§]

[†]Research and Development Center, Bando Chemical Industries, Ltd., Kobe 650-0047, Japan

[‡]Hyogo-Prefectural Synchrotron Radiation Nanotechnology Laboratory, Tatsuno 679-5165, Japan

[§]Division of Materials Science and Engineering, Faculty of Engineering, Hokkaido University, Sapporo 060-8628, Japan

Supporting Information

**ABSTRACT:** The time dependence of small-angle X-ray scattering (SAXS) curves for silver nanoparticle formation was followed in situ at a time resolution of 0.18 ms, which is 3 orders of magnitude higher than that used in previous reports (ca. 100 ms). The starting materials were silver nitrate solutions that were reacted with reducing solutions containing trisodium citrate. The SAXS analyses showed that silver nanoparticles were formed in three distinct periods from a peak diameter of ca. 0.7 nm (corresponding to the size of a $Ag_{13}$ cluster) during the nucleation and the early growth period. The $Ag_{13}$ clusters are most likely elementary clusters that agglomerate to form silver nanoparticles.

Silver and gold metal nanoparticles can be sintered on polymer films[1−4] and even paper[5] as a result of melting point depression and size effects[1,2,4,6] and thus have attracted much attention as electro-conductive metallic inks for printed electronics.[2,4,7] Practical applications would require specific particle size distributions to enable fabrication of closely packed layers of nanoparticles rather than monodispersed nanoparticles.[1,4] Therefore, a better understanding of the formation mechanism of noble-metal nanoparticles is needed to prepare desired diameter and size distribution formulations. Classical growth models state that particles are formed by means of monomer addition after a discrete nucleation period,[8] while recent studies have shown that silver and gold nanoparticles are formed via a complex pathway that includes a broad nucleation period with a simultaneous particle growth period.[9−12] Generally, it can be considered that a cluster consisting of several atoms rather than a single atom acts as an elementary species that determines monomer addition and particle growth. Silver and gold metal clusters along with the full-shell clusters, in which a central atom is surrounded by shells of atoms to form an icosahedron, are thought to be thermodynamically stable.[13,14] The cluster sizes of the first- and second-full-shell clusters, $Ag_{13}$ and $Ag_{55}$, are estimated to be 0.7 and 1.2 nm,[15] respectively. The existence of the $Ag_{13}$ cluster has not been clarified in previous literature, unlike $Au_{13}$ clusters,[14,16] although attractive magnetic properties of the $Ag_{13}$ cluster have been widely discussed with the help of computational science.[17]

Small-angle X-ray scattering (SAXS) could be an effective technique for evaluating in situ size distributions of nanoparticles because it has the potential for statistical processing of a very large number of particles.[11,18,19] Previous studies, however, have not clearly established the size of elementary silver clusters because the determination of this size would require in situ observation at an extremely high time resolution (ca. a few milliseconds). Detailed discussion of the formation mechanism with SAXS would also require a specialized apparatus rather than batch-type conditions to completely fix the onset of the formation of all particles. In this work, we have used a custom-fabricated one-direction-of-flow reactor cell to obtain in situ SAXS curves at high time resolutions of 0.18 ms, which is 3 orders of magnitude higher than those used in previous studies[11,18] (ca. 100 ms). By analyzing the time dependence of the in situ SAXS curves for silver nitrate solutions reacting with reducing solutions containing trisodium citrate[20] as a weak dispersant, we discuss fine details of the sizes of the elementary clusters formed and the mechanism of silver nanoparticle formation in an aqueous system.

Conventional chemical reduction in an aqueous system was used for the examination of the formation of silver nanoparticles. A one-direction-of-flow reactor cell made of poly(methyl methacrylate) resin equipped with polyimide thin-film windows and two injection flow channels enabled mixing of two influent solutions and a single efficient flow channel. The silver ion solution and a reducing solution were fed at equal flow rates (120 mL $min^{-1}$) into a Y-junction to allow mixing under turbulent flow conditions. The SAXS measurements were carried out at beamline BL08B2 at the SPring-8 synchrotron radiation facility in Japan. The reactor cell was set on a vertically movable stage to control the X-ray irradiation position axially from the mixing point. From the mixing point (defined as the point of origin, 0 ms reaction time), a distance of 1 mm along the reactor cell corresponded to a reaction time of 0.393 ms on the basis of the given flow rate. A maximum time resolution of 0.18 ms was possible for a vertical beam size of 0.23 mm. The technique of using a flow reactor with a Y-junction requires considerable amounts of silver solution to enable in situ measurements at the given time resolutions. This means that the cost of each experiment was high, and thus, the number of experiments was limited. The two-dimensional scattering images detected on the X-ray imaging plate were converted to one-dimensional scattering curves giving the scattering vector ($q$) dependence of the scattering intensities by azimuthal integration and subtraction of each scattering curve of the solution including all chemicals except

**Received:** March 28, 2011
**Published:** August 17, 2011

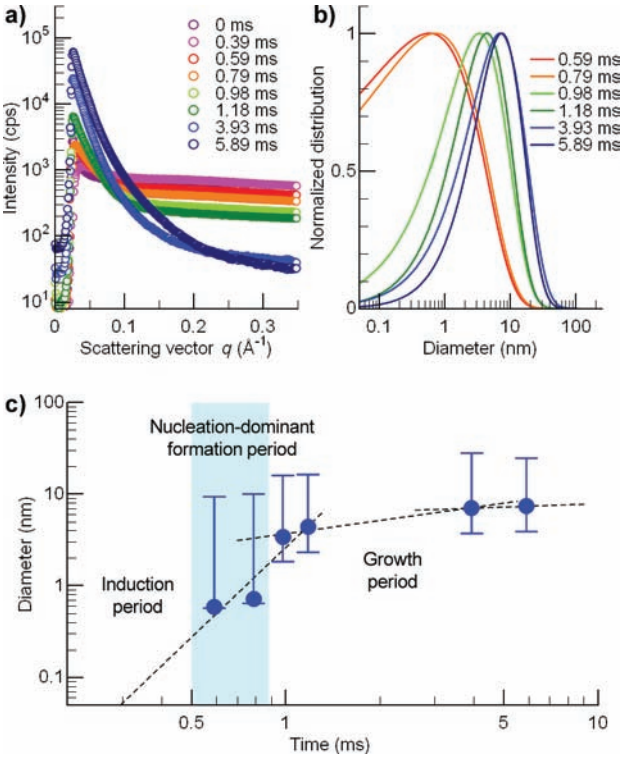


**Figure 1.** Time dependence of the formation of silver clusters and nanoparticles. (a) SAXS curves measured in the custom-fabricated one-direction-of-flow reactor cell at various times. (b) Particle size distributions fitted with the SAXS curves. Fitting of the SAXS scattering curves is described in Table S1 and Figure S2. (c) Time dependence of the peak diameter (●) and the particle diameters at volume fractions of 10 and 90% (error bars). Proposed periods of the silver nanoparticle formation process are overlaid. Dashed lines show power approximation fits to help distinguish the growth rate periods.

for the silver ions. The size distribution of the silver nanoparticles and clusters was determined by curve fitting with a Γ distribution function.[21] Detailed materials and methods are available in the Supporting Information (SI).

The time dependence of the scattering intensities of the SAXS curves and the particle size distributions fitted with the intensities as well as an analysis of the time dependence of the nanoparticles and clusters are shown in Figure 1 (also see Table S1 and Figure S2 in the SI). The decrease in the scattering intensities at $q <$ ca. 0.025 $Å^{-1}$ in all curves (Figure 1a) was due to shielding of the beam stopper, so these areas can be excluded from the discussion.

The scattering curves were almost flat and constant at reaction times of 0 and 0.39 ms. This means that the $q$ ranges may not reach the Porod region because the particles are too small or absent at the given reaction times. Curve fittings at short reaction times of 0 and 0.39 ms had high uncertainties and are not displayed (Figure S2a,b). In the induction period, the reduction process from $Ag^+$ ions to $Ag^0$ atoms is most likely taking place, but the nucleation has not been initiated. Still, even at this high time resolution, it was not possible to describe the progress of the reduction process completely with the SAXS measurements.

The gradients of the scattering curves increased distinctly at reaction times greater than 0.59 ms. The scattering curves at the reaction times could be well-fitted throughout the whole $q$ range (Figure S2c−h). It is probable that there is a trigger for the onset of nucleation of silver clusters and nanoparticles between 0.39 and 0.59 ms, and the onset becomes clear at 0.59 ms.

At reaction times of 0.59 and 0.79 ms, when nucleation had started according to the increase in the particle sizes, the peak diameters were 0.58 and 0.71 nm, respectively, indicating that the nucleation of $Ag_{13}$ clusters (which have a diameter of 0.7 nm) predominated at the 0.59 and 0.79 ms reaction times. On the other hand, the observed larger diameters in the size distributions at 0.59 and 0.79 ms (>10 nm) are evidence that the growth of silver nanoparticles had started along with the nucleation. This nucleation-dominant formation period, in which $Ag_{13}$ clusters were nucleated and consumed in the simultaneous formation and growth of silver nanoparticles, was almost certainly not continuing at 0.98 ms, as shown by volume fractions that were ca. 0.7 nm in size and considerably decreasing with reaction time. Although the limited experiments performed in this study prevent a quantitative discussion of whether all silver atoms went through $Ag_{13}$ clusters, the particle size distributions show that $Ag_{13}$ clusters are the dominant species during the nucleation-dominant formation period.

A distinct change in the particle size distributions appeared as an abrupt increase in the peak diameters at and later than the reaction time of 0.98 ms. The peak diameters of the silver nanoparticles increased from 0.71 to 3.36 nm at reaction times between 0.79 and 0.98 ms, and the 10% volume fraction of particles was 1.82 nm at 0.98 ms, suggesting that $Ag_{13}$ clusters were depleted at 0.98 ms. The nucleation of $Ag_{13}$ clusters seemed to be completely terminated at 0.98 ms, and the growth of silver nanoparticles predominated after 0.98 ms. The main process in this growth period is most likely coalescence of smaller silver nanoparticles that were formed mainly by agglomeration of $Ag_{13}$ clusters during the previous nucleation-dominant formation period. Alternatively, there is the possibility that silver nanoparticles grew continuously by the addition of silver atoms reduced in the early period on $Ag_{13}$ clusters. In that case, silver nanoparticle formation would grow via $Ag_{55}$ clusters, which are the next full-shell clusters and have a diameter of 1.2 nm. However, the fraction of particles having diameters of ca. 1.2 nm was not dominant during the period between 0.79 and 0.98 ms. Although it is not possible to ignore completely the possible presence and contribution of $Ag_{55}$ clusters in the particle formation process because a small volume fraction of particles with diameters of ca. 1.2 nm did exist, the silver atoms reduced can be assumed to take part preferentially in the immediate nucleation of $Ag_{13}$ clusters rather than remaining as-is for an extended period awaiting consumption in the formation of $Ag_{55}$ clusters. Therefore, it can be hypothesized that silver nanoparticles grow mainly via $Ag_{13}$ clusters rather than clusters of other sizes. Thus, $Ag_{13}$ clusters play an important role as an elementary cluster in the formation of the silver nanoparticles.

The peak diameters gradually increased from 3.36 nm at 0.98 ms to 6.95 nm at 3.93 ms, where larger particles were over 20 nm in diameter; at the reaction time of 5.89 ms, the peak diameters showed only a slight increase (Figure 1c). This means that the growth process was substantially complete at 3.93 ms. At 3.93 and 5.89 ms, 90% of the volume fraction was over 3 nm. On the other hand, the particle size distribution narrowed slightly at 5.89 ms in comparison with that at 3.93 ms, which may be attributed to a relaxation or rearrangement of transient aggregated larger particles during the period after 3.93 ms. Further elucidation of the relaxation process requires additional experiments and a greater number of data.

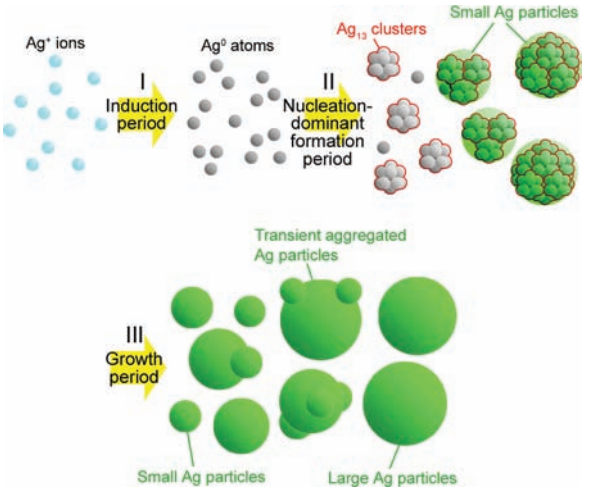


**Figure 2.** Proposed mechanism of silver nanoparticle formation via $Ag_{13}$ clusters. Silver nanoparticles are formed through (I) an induction period during which $Ag^+$ ions are reduced to $Ag^0$ atoms; (II) a nucleation-dominant formation period during which $Ag_{13}$ clusters are nucleated and simultaneously consumed in silver nanoparticle formation; and (III) a growth period during which larger silver nanoparticles are formed by coalescence and aggregation of smaller silver nanoparticles.

The formation of silver nanoparticles in an aqueous system proceeded during a very short reaction time of ca. 6 ms and seemed to consist of three distinct periods, as proposed in Figure 1c and shown schematically as a formation mechanism in Figure 2. After a short induction period in which silver ions are reduced, $Ag_{13}$ clusters are actively formed, and small silver nanoparticles are subsequently formed mainly by agglomeration of $Ag_{13}$ clusters (nucleation-dominant formation period). The formation of silver nanoparticles seems to have no discrete nucleation period according to the time scales and methods used in this work. The $Ag_{13}$ clusters are practically consumed during the nucleation-dominant formation period. Particle growth occurs by coalescence and aggregation of the small silver nanoparticles, resulting in larger silver nanoparticles (growth period).

In summary, the SAXS results obtained here show that silver nanoparticles are formed via three distinct periods within 6 ms and that the diameter of the silver nanoparticles increases mainly via clusters with a diameter of ca. 0.7 nm, corresponding to the size of a $Ag_{13}$ cluster. $Ag_{13}$ clusters play an important role as an elementary cluster in the formation of silver nanoparticles.

## ■ ASSOCIATED CONTENT

**Ⓢ Supporting Information.** Experimental procedures. This material is available free of charge via the Internet at http://pubs.acs.org.

## ■ AUTHOR INFORMATION

**Corresponding Author**
masafumi.takesue@bando.co.jp

## ■ ACKNOWLEDGMENT

This study was carried out at SPring-8 under proposal no. 2008B3300 through CREATE organized by the Hyogo Prefecture and funded by JST, for development of a common ground of a nanoparticle composite. We thank Prof. Emeritus Katsuhiko Nakamae (Kobe University) for pushing this study forward, Masanori Kiyoi (Bando Chemical) for designing the feeding apparatus, and Prof. Richard L. Smith, Jr. (Tohoku University) for many valuable discussions. T.Y. is grateful for the partial financial support through a Grant-in-Aid for Scientific Research (B) (21310072) from JSPS and a Grant-in-Aid for Scientific Research in Priority Area (Strong Photon−Molecule Coupling Fields for Chemical Reactions (470, 21020010) from MEXT, Japan.

## ■ REFERENCES

(1) Moon, K.-S.; Dong, H.; Maric, R.; Pothukuchi, S.; Hunt, A.; Li, Y.; Wong, C. P. *J. Electron. Mater.* **2005**, *34*, 168–175.
(2) Sivaramakrishnan, S.; Chia, P.-J.; Yeo, Y.-C.; Chua, L.-L.; Ho, P. K.-H. *Nat. Mater.* **2007**, *6*, 149–155.
(3) Klajn, R.; Bishop, K. J. M.; Fialkowski, M.; Paszewski, M.; Campbell, C. J.; Gray, T. P.; Grzybowski, B. A. *Science* **2007**, *316*, 261–264.
(4) Perelaer, J.; Hendriks, C. E.; de Laat, A. W. M.; Schubert, U. S. *Nanotechnology* **2009**, *20*, No. 165303.
(5) Magdassi, S.; Grouchko, M.; Berezin, O.; Kamyshny, A. *ACS Nano* **2010**, *4*, 1943–1948.
(6) (a) Jin, R.; Cao, Y. C.; Hao, E.; Métraux, G. S.; Schatz, G. C.; Mirkin, C. A. *Nature* **2003**, *425*, 487–490. (b) Tao, A.; Sinsermsuksakul, P.; Yang, P. *Nat. Nanotechnol.* **2007**, *2*, 435–440.
(7) (a) Shimoda, T.; Matsuki, Y.; Furusawa, M.; Aoki, T.; Yudasaka, I.; Tanaka, H.; Iwasawa, H.; Wang, D.; Miyasaka, M.; Takeuchi, Y. *Nature* **2006**, *440*, 783–786. (b) Gamerith, S.; Klug, A.; Scheiber, H.; Scherf, U.; Moderegger, E.; List, E. J. W. *Adv. Funct. Mater.* **2007**, *17*, 3111–3118. (c) Ahn, B. Y.; Duoss, E. B.; Motala, M. J.; Guo, X.; Park, S.-I.; Xiong, Y.; Yoon, J.; Nuzzo, R. G.; Rogers, J. A.; Lewis, J. A. *Science* **2009**, *323*, 1590–1593. (d) Rogers, J. A.; Someya, T.; Huang, Y. *Science* **2010**, *327*, 1603–1607.
(8) LaMer, V. K.; Dinegar, R. H. *J. Am. Chem. Soc.* **1950**, *72*, 4847–4854.
(9) Biswas, K.; Varghese, N.; Rao, C. N. R. *Small* **2008**, *4*, 649–655.
(10) Zheng, H.; Smith, R. K.; Jun, Y.-W.; Kisielowski, C.; Dahmen, U.; Alivisatos, A. P. *Science* **2009**, *324*, 1309–1312.
(11) Polte, J.; Erler, R.; Thünemann, A. F.; Sokolov, S.; Ahner, T. T.; Rademann, K.; Emmerling, F.; Kraehnert, R. *ACS Nano* **2010**, *4*, 1076–1082.
(12) (a) Richards, V. N.; Rath, N. P.; Buhro, W. E. *Chem. Mater.* **2010**, *22*, 3556–3567. (b) Meli, L.; Green, P. F. *ACS Nano* **2008**, *2*, 1305–1312.
(13) *Nanoparticles*; Schmid, G., Ed.; Wiley-VCH: Weinheim, Germany, 2000.
(14) Schmid, G. *Chem. Soc. Rev.* **2008**, *37*, 1909–1930.
(15) (a) Amano, C.; Niina, H.; Mikami, Y. *THEOCHEM* **2009**, *904*, 64–68. (b) Harb, M.; Rabilloud, F.; Simon, D. *Phys. Chem. Chem. Phys.* **2010**, *12*, 4246–4254.
(16) Shichibu, Y.; Konishi, K. *Small* **2010**, *6*, 1216–1220.
(17) (a) Pereiro, M.; Baldomir, D.; Arias, J. E. *Phys. Rev. A* **2007**, *75*, No. 063204. (b) Piotrowski, M. J.; Piquini, P.; Da Silva, J. L. F. *Phys. Rev. B* **2010**, *81*, No. 155446.
(18) (a) Abécassis, B.; Testard, F.; Spalla, O.; Barboux, P. *Nano Lett.* **2007**, *7*, 1723–1727. (b) Abécassis, B.; Testard, F.; Spalla, O. *Phys. Rev. Lett.* **2008**, *100*, No. 115504.
(19) (a) Jensen, H.; Bremholm, M.; Nielsen, R. P.; Joensen, K. D.; Pedersen, J. S.; Birkedal, H.; Chen, Y.-S.; Almer, J.; Søgaard, E. G.; Iversen, S. B.; Iversen, B. B. *Angew. Chem., Int. Ed.* **2007**, *46*, 1113–1116. (b) Lee, G.-W.; Jin, K. S.; Kim, J.; Bae, J.-S.; Yeum, J. H.; Ree, M.; Oh, W. *Appl. Phys. A: Mater. Sci. Process.* **2008**, *91*, 657–661. (c) Plech, A.; Kotaidis, V.; Siems, A.; Sztucki, M. *Phys. Chem. Chem. Phys.* **2008**, *10*, 3888–3894. (d) Bremholm, M.; Felicissimo, M.; Iversen, B. B. *Angew. Chem., Int. Ed.* **2009**, *48*, 4788–4791.

(20) (a) Mühlpfordt, H. *Experientia* **1982**, *38*, 1127–1128. (b) Tsai, C. Y.; Lee, D. S.; Tsai, Y. H.; Chan, B.; Luh, T. Y.; Chen, P. J.; Chen, P. H. *Mater. Lett.* **2004**, *58*, 2023–2026. (c) Chen, H. M.; Hsin, C. F.; Liu, R.-S.; Lee, J.-F.; Jang, L.-Y. *J. Phys. Chem. C* **2007**, *111*, 5909–5914. (d) Mpourmpakis, G.; Vlachos, D. G. *Phys. Rev. Lett.* **2009**, *102*, No. 155505.

(21) (a) Nagao, O.; Harada, G.; Sugawara, T.; Sasaki, A.; Ito, Y. *Jpn. J. Appl. Phys.* **2004**, *43*, 7742–7746. (b) Yao, H.; Miki, K.; Nishida, N.; Sasaki, A.; Kimura, K. *J. Am. Chem. Soc.* **2005**, *127*, 15536–15543. (c) Nishida, N.; Yao, H.; Ueda, T.; Sasaki, A.; Kimura, K. *Chem. Mater.* **2007**, *19*, 2831–2841.